Research on Engineering Structures & Materials
www.jresm.org
Research Group

Research Article

Experimental study on the impact of elevated temperature exposure from fire on low-strength concrete quality

Muhajir [1,a], Tamrin [*,2,b], Mardewi Jamal [2,c]

[1]*Master of Civil Engineering, Mulawarman University, Samarinda, Indonesia*
[2]*Department of Civil Engineering, Mulawarman University, Samarinda, Indonesia*

Article Info

Article History:

Received 28 June 2026

Accepted 22 Aug 2026

Keywords:

Low-strength concrete;
Elevated temperature;
Fire damage;
Residual compressive strength;
Structural assessment

Abstract

Concrete remains the most widely used construction material for buildings and infrastructure because of its high compressive strength, durability, and cost-effectiveness. However, fire exposure can significantly impair its structural performance through moisture loss, thermal cracking, spalling, and the degradation of cement hydration products. Although the fire behavior of normal- and high-strength concrete has been extensively studied, experimental evidence on low-strength concrete (f'c ≈ 10–15 MPa), which is still common in older buildings and public facilities in Indonesia, remains limited. This study investigates the effects of elevated temperatures on the residual compressive strength and visible deterioration of low-strength concrete with a target compressive strength of 12.5 MPa. A narrative literature review was combined with controlled laboratory experiments using cylindrical specimens exposed to temperatures of 200°C, 300°C, 400°C, and 500°C. Residual compressive strength was determined through standard compression testing, while surface deterioration was assessed by visual inspection. The results showed progressive strength reductions of 4.8%, 13.6%, 28.0%, and 42.4%, respectively, with one-way ANOVA confirming a significant effect of temperature on residual compressive strength ($F(4,10) = 1015.07$, $p < 0.001$). More severe deterioration was observed above 300°C, characterized by color changes, crack propagation, and friable concrete surfaces. These findings provide practical experimental evidence to support post-fire structural assessment and decision-making for the repair, strengthening, or demolition of low-strength concrete structures in Indonesia.

1. Introduction

Indonesia is experiencing a growing threat from building fires. According to data from Statistics Indonesia [1], structural fire incidents have been increasing annually, resulting in substantial economic losses and severe damage to public infrastructure. Beyond the immediate destruction caused by fire, one of the most critical engineering challenges is determining whether a fire-damaged concrete structure remains serviceable, requires strengthening, or must be demolished.

Concrete is the most widely used material in buildings, bridges, and infrastructure due to its high compressive strength, durability, and relatively low production cost [2,3]. Despite these advantages, concrete remains vulnerable to elevated temperatures. Under high-temperature conditions, concrete experiences progressive deterioration caused by moisture evaporation, thermal incompatibility between cement paste and aggregates, decomposition of hydration products, and the development of internal cracking [2–5]. Severe exposure may result in spalling, brittleness, and significant reductions in residual compressive strength, ultimately compromising structural performance [3,4,22].

*Corresponding author: fts_tamrin@yahoo.com
[a]orcid.org/0009-0002-8372-6212; [b]orcid.org/0009-0005-7880-9103; [c]orcid.org/0009-0002-3192-5236
DOI: http://dx.doi.org/10.17515/resm2026-1804ma0628rs

Previous studies have demonstrated that elevated temperatures significantly affect both the mechanical properties and microstructural integrity of concrete. Shahraki et al. [2] developed probabilistic models for predicting residual compressive strength after fire exposure, while Kakae et al. [3] investigated the physical and thermal degradation mechanisms of heated concrete. Other researchers have evaluated post-fire structural behavior using destructive and non-destructive approaches, including residual compressive strength testing, ultrasonic pulse velocity, rebound hammer methods, and numerical modelling [5–8]. At elevated temperatures above approximately 400°C, the decomposition of portlandite ($Ca(OH)_2$) and progressive depolymerization of calcium silicate hydrate (C–S–H) substantially reduce concrete stiffness and strength [2,3,22–24]. Spalling phenomena and thermal cracking become more severe, especially in concrete subjected to rapid heating or containing dense microstructures [9–13].

However, most previous investigations focused on normal-strength or high-strength concrete commonly used in developed countries [2,4,22–24]. Experimental data concerning low-strength concrete (f'c ≈ 10–15 MPa), which is still widely found in older school buildings, residential structures, and community facilities in Indonesia, remain limited. This constitutes a significant gap in the literature: post-fire assessment guidelines and probabilistic strength models developed for higher-grade concrete may not be directly applicable to the lower-grade concrete stock that predominates in public buildings across developing nations.

Fig. 1. Field documentation of the fire at SDN 022 Penajam (31 January 2024), which motivated the present experimental investigation. The left photograph shows the building during the active fire, while the right photograph shows the post-fire condition after fire suppression, including extensive fire damage and debris clearance prior to structural assessment. Photos: Field documentation by the authors

The present study addresses this research gap by experimentally investigating the residual compressive strength and visible surface degradation of low-strength concrete exposed to temperatures of 200°C, 300°C, 400°C, and 500°C. The study is motivated by a real fire incident at SD Negeri 022 Penajam (Sekolah Dasar Negeri; a government-operated state primary school), East Kalimantan, Indonesia. The three objectives of this study are: (1) to evaluate the residual compressive strength of low-strength concrete after exposure to elevated temperatures; (2) to document visible thermal damage characteristics including color change and surface cracking; and (3) to assess the implications of strength degradation for post-fire structural safety evaluation in the Indonesian context.

Consistent with these objectives, the study tests the following hypotheses: (H1) the residual compressive strength of low-strength concrete (f'c ≈ 12.5 MPa) decreases significantly with increasing exposure temperature across the 200–500°C range; (H2) the rate of strength loss is not linear but accelerates once exposure temperature exceeds approximately 300°C, consistent with the onset of calcium hydroxide dehydration reported for higher-grade concrete; and (H3) visible surface deterioration becomes progressively more severe with increasing temperature and strength loss, such that visual inspection may provide a preliminary, though not definitive, indication of thermal damage severity.

Unlike previous studies that predominantly investigated normal- and high-strength concrete, the present study specifically examines low-strength concrete (approximately 12.5 MPa), which remains widely used in older Indonesian public buildings. The study further integrates experimental laboratory testing with observations from an actual fire incident, thereby providing locally relevant reference data for post-fire structural assessment in developing countries.

2. Material and Methods

2.1 Temperature Gradient

Concrete building elements consist of aggregates bound by hydrated cement paste, reinforced or prestressed with steel. In compartment fire conditions, gas temperatures increase rapidly, often reaching a fully developed phase before gradually decreasing during cooling. During fire exposure, steep thermal gradients develop within structural members, accompanied by moisture migration and internal thermal stresses. These processes induce physical and chemical changes that progressively reduce stiffness, strength, and bond performance while increasing the risk of cracking and spalling [3,15,22,26].

The severity of thermal damage is influenced by peak temperature, heating duration, cooling rate, moisture condition, aggregate mineralogy, member dimensions, and mechanical restraint during heating [2,3,22]. At relatively low temperatures (below approximately 200°C), deterioration is mainly associated with evaporation of free and adsorbed water from capillary pores. As temperatures exceed 300°C, degradation becomes increasingly severe [2,3,20–25].

2.2 Temperature-Dependent Damage Mechanisms

Hygral Effects (20–200°C). Free water evaporates and bound water begins to migrate. In low-permeability, moist concrete subjected to rapid heating, pore pressure can build up, causing microcracking and potentially explosive spalling [3,9,10,21]. Dehydration of Hydrates (≈105–400°C). C–S–H, ettringite, and portlandite lose bound water. The matrix becomes less continuous, interfacial transition zone (ITZ) debonding increases, and stiffness tends to degrade earlier and faster than compressive strength [2,3,20,24]. Chemical Decomposition (400–800°C). Portlandite decomposes at approximately 400–600°C, causing a marked reduction in stiffness and compressive strength [2,3,23]. C–S–H depolymerization intensifies beyond 600°C, severely reducing cohesion [2]. Aggregate transformations, including the α–β quartz transition occurring near 573°C, introduce additional thermal cracking [2,3,30].

Thermal Mismatch and Structural Restraint. Different thermal expansion coefficients of paste, aggregates, and steel induce shear and tension at the ITZ. Under sustained gravity loads and structural restraint, transient thermal creep accelerates inelastic strains, amplifying deflections and damage [2,3,26]. Spalling in Building Elements. Spalling arises from combined pore-pressure and thermal-stress mechanisms, promoted by dense or high-strength mixes, high moisture content, thin concrete covers, rapid heating rates, and high axial load [9–13,21]. Polypropylene fibres and pre-drying reduce explosive spalling risk by improving vapor pressure dissipation during heating [9–13].

2.3 Residual Properties Relevant to Building Safety

- Compressive Strength: Declines nonlinearly with temperature: often modest up to 200–300°C, then accelerating markedly beyond 400°C [2,22,23]. Hertz [28] proposed a bilinear model widely adopted in structural fire design.
- Elastic Modulus: Degrades faster than strength; serviceability (deflection, crack width) can govern even when residual strength seems acceptable [2,4,22]. Buchanan and Abu [26]

emphasize that deformation-based checks are critical in fire-exposed structures. Bond to Reinforcement. Cover cracking, spalling, matrix softening, and thermal mismatch reduce bond and anchorage; slip at laps and anchors becomes critical in post-fire assessment [4,27].

- Low-Strength Concrete Behavior: Low-strength concretes (f'c ≈ 10–15 MPa) typical of older Indonesian buildings may have higher initial porosity, reducing explosive spalling risk compared to dense high-strength concrete [9,23]. However, elastic modulus and tensile capacity still deteriorate rapidly beyond 300–400°C, making axially loaded columns and walls particularly vulnerable [2,9,23].

2.4 Research Gap and Contribution of the Present Study

Although numerous studies have investigated fire-damaged concrete, most prior research focused primarily on normal-strength or high-strength concrete (f'c ≥ 25 MPa) commonly used in developed countries [2,4,22–25,27–30]. These strength classes differ substantially from the low-strength concrete (f'c ≈ 10–15 MPa) that still predominates in older school buildings, residential structures, and community facilities across Indonesia. Because degradation mechanisms, porosity characteristics, and residual strength trajectories differ between concrete grades, direct extrapolation from international high-strength datasets to this lower-grade stock introduces non-trivial uncertainty in post-fire decision-making.

A second gap lies in contextualization. Most previous investigations were conducted under idealized laboratory conditions without reference to actual fire incidents in Indonesian public buildings. Nationally applicable strength models and post-fire assessment protocols have not been validated for the specific concrete grades and construction practices encountered in Indonesian infrastructure.

The present study directly addresses both gaps by: (i) experimentally quantifying the residual compressive strength and visible thermal damage of low-strength concrete (f'c ≈ 12.5 MPa) across the range 200–500°C; and (ii) contextualizing the findings using a documented fire incident at SD Negeri 022 Penajam, East Kalimantan, Indonesia. The results are intended to provide locally relevant empirical reference data supporting post-fire structural assessment decisions for public buildings constructed with lower-grade concrete in Indonesia.

2.5 Materials and Sample Preparation

Since it was not feasible to retrieve concrete samples directly from the fire-damaged building, new specimens were produced in the laboratory using a mix design estimated to match the original structure's concrete. The mix was selected based on the construction era and visual inspection of non-fire-damaged sections, which suggested the structure was built to Class I concrete specifications targeting a characteristic compressive strength of approximately 10–15 MPa with a water-to-cement ratio (w/c) of 0.6. Mix proportions by mass used Portland Composite Cement (PCC type), fine aggregate (local river sand from Kalimantan, fineness modulus ≈ 2.8, unit weight 2.54 g/cm^3), coarse aggregate (crushed basaltic gravel from Palu, Central Sulawesi, maximum size 20 mm, unit weight 2.55 g/cm^3, abrasion resistance 23%), and water. Palu aggregates are of basaltic origin and are widely used for concrete in Indonesia; they offer higher resistance to alkali-silica reaction compared to aggregates from some areas in East Kalimantan and have been characterized in previous studies conducted at Mulawarman University [31].

Freshly mixed concrete was cast into cylindrical moulds measuring 15 cm in diameter and 30 cm in height (standard SNI 1974:2011 dimensions) [14]. Each cylinder was left in the mold for 24 hours for initial setting, then demolded and moist-cured at room temperature (approximately 27°C) until reaching the testing age of 28 days. A total of 15 cylindrical specimens were prepared and divided into five treatment groups (n = 3 per group): a control group at room temperature (~27°C) and four heated groups exposed to 200°C, 300°C, 400°C, and 500°C, respectively.

Table 1. Concrete mix design (job mix formula) used for laboratory specimens

No.	Material	Specification	Quantity per m^3 (kg)	Quantity per batch* (kg)	Role in Mix
1	Portland Composite Cement (PCC)	SNI 7064:2014; Type PCC	276	4.14	Binder
2	Fine Aggregate (river sand)	FM ≈ 2.8; SSD; unit wt 2.54 g/cm^3; local Kalimantan River sand	799	11.99	Fine filler
3	Coarse Aggregate (crushed gravel)	Max. size 20 mm; SSD; unit wt 2.55 g/cm^3; abrasion 23%; basaltic, from Palu, Central Sulawesi [31]	1,093	16.40	Coarse filler
4	Water	Clean tap water; potable	166	2.49	Hydration medium
	Water-to-Cement Ratio (w/c)	Target ≤ 0.60	0.60	0.60	Workability / strength control
	Cement: Sand: Gravel ratio	By mass	1: 2.9: 3.96	-	Mix proportioning
	Target f′c (28-day)	Class I concrete (SNI)	≈ 12.5 MPa	-	Structural grade baseline

** Batch volume = 15 liters (sufficient for three ?15×30 cm cylinders). FM = fineness modulus; SSD = saturated surface-dry condition. Quantities rounded to nearest 0.01 kg. Mix proportioning follows SNI 03-2834-2000 method for normal concrete*

2.6 High-Temperature Treatment (Fire Simulation)

After reaching 28 days of age, specimens assigned to the high-temperature groups were heated using a modified steel-drum furnace fabricated specifically for this study (Figure 2a), rather than a standard laboratory muffle furnace. The apparatus consisted of a cylindrical steel drum lined internally with refractory insulation and fitted with electric heating elements, enabling controlled and reasonably uniform heating of the enclosed specimens. A calibrated thermocouple was inserted at specimen mid-height and connected to a digital temperature controller to monitor and regulate internal chamber temperature throughout the heating phase; specimen surface temperature was independently cross-checked using a non-contact infrared thermometer (Figure 2c). Heating was carried out at a controlled rate of approximately 5°C per minute to prevent thermal shock, consistent with recommendations in the literature [2,3]. Once the target temperature was achieved, it was maintained (soak period) for approximately 2 hours to promote thermal equilibrium throughout the specimen volume before the heating elements were switched off.

Following the soak period, specimens were allowed to cool naturally inside the closed furnace chamber to approximately 100°C before removal, and were then cooled further in ambient laboratory air (approximately 27°C) to room temperature; no water quenching was applied at any stage. Visual changes were documented using a standardized rubric: (i) color change — coded as normal grey, reddish, or whitish; (ii) crack type — coded as none, hairline, micro, or macro/wide; and (iii) overall condition — coded as intact, friable, or spalled. All visual assessments were conducted independently by two researchers, with discrepancies resolved by consensus.

2.7 Compressive Strength Testing

Compressive strength testing was performed on each cooled cylinder using a hydraulic compression machine (capacity approximately 2,000 kN), following SNI 1974:2011 [14]. Each cylindrical specimen was positioned vertically between the loading plates, and a steadily increasing load at approximately 0.25 MPa per second was applied until failure. The maximum load at failure was recorded, and compressive strength (f'c) was calculated by dividing the load by the cross-sectional area.

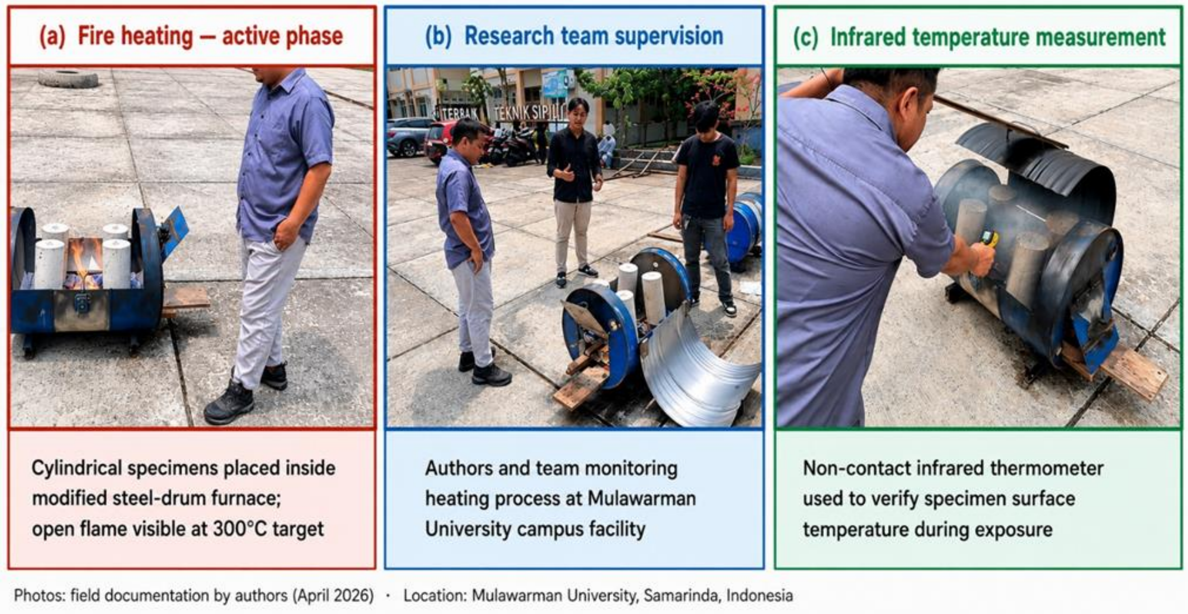

Fig. 2. Fire simulation setup and temperature monitoring: (a) cylindrical specimens inside modified steel-drum furnace during active heating phase at 300°C target; (b) research team supervising the heating process at Mulawarman University campus; (c) non-contact infrared thermometer used to verify specimen surface temperature during exposure. Photos: field documentation by authors (April 2026)

2.8 Data Analysis and Structural Feasibility Criteria

The primary endpoint was mean residual compressive strength (MPa) at each temperature level. Strength Loss (%) = [(12.5 − Residual) / 12.5] × 100. Descriptive statistics (mean and range) are reported for each group. A one-way ANOVA was used to test the overall effect of temperature on residual compressive strength ($\alpha = 0.05$). Where significant, Tukey's HSD post-hoc test was applied. All analyses were performed using IBM SPSS Statistics v26. Given the small within-group sample size ($n = 3$), the normality assumption could not be rigorously verified using formal tests such as Shapiro–Wilk, which have very limited power at this sample size; no evidence of outliers or skew was observed in the raw data (Table 3). The homogeneity-of-variance assumption was formally tested using Levene's test and was not violated ($F = 0.08$, $p = 0.988$; see Section 3.1). Individual specimen-level compressive strength data underlying Table 2 are provided in Table 3.

Residual strength values were evaluated against indicative structural feasibility thresholds [2,4,15,26]: if post-fire concrete retains strength with no greater than 20–25% reduction, the structure may be considered serviceable with minor repair; if the strength loss exceeds 50% or the remaining strength falls below the load-bearing threshold, the structure is deemed unsafe. These percentages are used only as indicative material-level screening criteria and should not be interpreted as universal structural acceptance or rejection limits. Final safety decisions must also incorporate reinforcement condition, load redistribution capacity, member-level structural analysis, and professional engineering judgment.

2.9 Ultrasonic Pulse Velocity (UPV) Testing

To complement the destructive compressive strength testing with a non-destructive assessment, ultrasonic pulse velocity (UPV) measurements were additionally performed following the direct (cross-probing) transmission procedure of ASTM C597-16 [40]. Transducers were placed on the two opposite circular faces of the 150 × 300 mm cylindrical specimens (path length L = 0.3 m), and pulse transit time was recorded for the unheated control and each heated group (200°C, 300°C, 400°C, and 500°C), matching the compressive strength testing matrix in Table 2. Three repeat transit-time readings were taken for each group and averaged to obtain a representative pulse velocity, V = L/T. Unlike the compressive strength testing, which used three independent specimens per group (Table 2), the UPV dataset reported here consists of repeated readings rather than independent specimen replication, and should therefore be interpreted as indicative of the group-level trend rather than as a statistically independent sample.

Concrete quality was graded from the measured pulse velocity using the classification of Whitehurst [41], widely adopted in NDT practice (V > 4.5 km/s: excellent; 3.5–4.5 km/s: good; 3.0–3.5 km/s: medium; 2.0–3.0 km/s: doubtful; < 2.0 km/s: poor). Consistent with IS 13311(Part 1):1992 guidance, UPV-based quality grading is treated as an indicator of relative uniformity and internal damage rather than as a direct, calibrated estimate of compressive strength, since the velocity–strength relationship is sensitive to aggregate type, moisture condition, and mix proportions and was not independently calibrated for this specific mix.

3. Results

3.1 Residual Compressive Strength

Mean residual compressive strength decreased monotonically with increasing temperature across all groups, as summarized in Table 2. Starting from a control mean of 12.5 MPa, strength declined to 11.9 MPa at 200°C (4.8% loss), 10.8 MPa at 300°C (13.6% loss), 9.0 MPa at 400°C (28.0% loss), and 7.2 MPa at 500°C (42.4% loss). Within-group variability was very low throughout (SD 0.10–0.17 MPa; maximum range 0.3 MPa), reflecting the tightly controlled thermal conditioning of the specimens; individual specimen values are provided in Table 3. The rate of strength decline accelerated notably above 300°C, likely due to the onset of thermally induced physicochemical changes such as $Ca(OH)_2$ decomposition and progressive microcracking [2,3]. The effect size was very large (partial $\eta^2 = 0.998$), indicating that temperature treatment accounted for essentially all of the variance in residual compressive strength observed among specimens.

Table 2. Mean residual compressive strength of low-strength concrete (f'c ≈ 12.5 Mpa, n = 3 per group) after high-temperature exposure

Temperature (°C)	Reference Control Strength (MPa)	Residual Strength, Mean ± Range (MPa)	Strength Loss (%)	Notes
25 (Control)	12.5	12.5 ± 0.2	—	Unheated baseline; ambient ~27°C
200	12.5	11.9 ± 0.2	4.8	Minor free-water loss; no visible cracking
300	12.5	10.8 ± 0.2	13.6	Onset of $Ca(OH)_2$ dehydration; early hairline cracks
400	12.5	9.0 ± 0.3	28.0	Accelerated $Ca(OH)_2$ decomposition; micro-cracking
500	12.5	7.2 ± 0.2	42.4	Severe microstructural damage; wide cracks

Note: All values represent the mean of n = 3 specimens per temperature group; individual specimen data are provided in Table 3. The range (maximum–minimum) within each group was ≤ 0.3 MPa, and the standard deviation ranged from 0.10 to 0.17 MPa. One-way ANOVA demonstrated a highly significant effect of temperature on residual compressive strength ($F(4,10) = 1015.07$, $p < 0.001$; $p = 5.4 \times 10^{-13}$; partial $\eta^2 = 0.998$). Levene's test confirmed that the assumption of homogeneity of variance was satisfied ($F = 0.08$, $p = 0.988$). Tukey's HSD post-hoc analysis indicated that all pairwise comparisons, including the control-versus-200°C comparison ($p < 0.001$), were statistically significant, reflecting the very low within-group variability achieved under the controlled experimental conditions. Nevertheless, given the relatively small sample size per group (n = 3), these findings should be interpreted with appropriate caution and regarded as evidence of a consistent temperature-dependent trend. Confirmation using larger sample sizes is recommended in future studies.

One-way ANOVA confirmed a statistically significant overall effect of temperature on residual compressive strength ($F(4,10) = 1015.07$, $p < 0.001$; $p = 5.4 \times 10^{-13}$). Levene's test indicated that the homogeneity-of-variance assumption was not violated ($F = 0.08$, $p = 0.988$). Tukey's HSD post-hoc tests identified statistically significant pairwise differences between every pair of groups, including between the control and the 200°C group ($p < 0.001$) as well as between the control and both the 400°C group ($p < 0.001$) and the 500°C group ($p < 0.001$). The very low within-group variability of the tightly controlled specimens (SD 0.10–0.17 MPa; Table 3) means that even the comparatively modest 4.8% reduction at 200°C was statistically distinguishable from the control condition, although its practical engineering significance remains limited compared with the much larger losses recorded at 400°C and above. Given the limited sample size ($n = 3$ per group), these results should still be interpreted as indicative of a strong, consistent temperature-dependent trend; larger-scale studies would be warranted to further substantiate the findings.

Table 3. Individual specimen residual compressive strength values underlying Table 2

Temperature (°C)	Specimen 1 (MPa)	Specimen 2 (MPa)	Specimen 3 (MPa)	Mean (MPa)	SD (MPa)
25 (Control)	12.6	12.4	12.5	12.5	0.10
200	11.8	12.0	11.9	11.9	0.10
300	10.7	10.8	10.9	10.8	0.10
400	8.8	9.1	9.1	9.0	0.17
500	7.1	7.2	7.3	7.2	0.10

Note: Individual specimen values are provided in response to reviewer requests for raw underlying data. SD = standard deviation. These values were used to compute the ANOVA, Tukey HSD, and Levene's test results reported above.

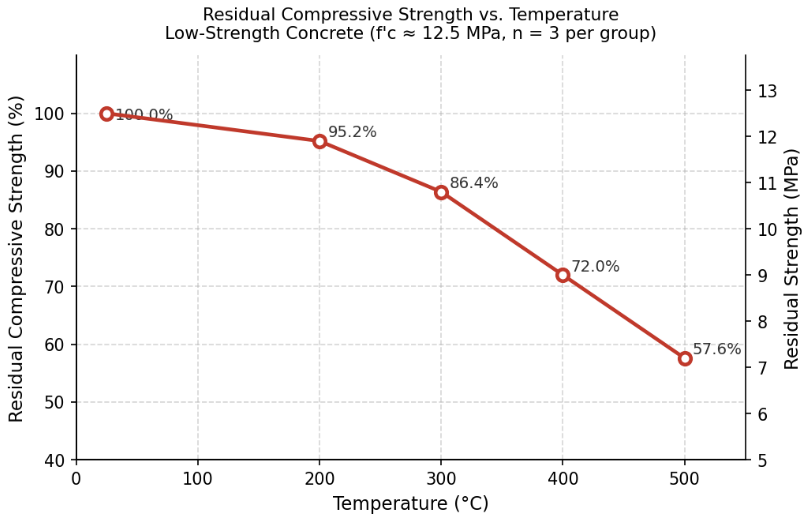

Fig. 3. Mean residual compressive strength (%) and absolute strength (MPa) of low-strength concrete (f'c ≈ 12.5 MPa) at each temperature exposure level. Each data point is the mean of n = 3 specimens. Error bars are not shown separately; within-group ranges did not exceed 0.3 MPa. The 100% baseline corresponds to the unheated control mean of 12.5 MPa

3.2 Visual Surface Changes

Visual observations were recorded at each temperature level using the standardized rubric (Figure 4). At 25°C (control), specimens appeared uniformly grey with a smooth, intact surface and no visible cracking or discoloration. At 200°C, minor color lightening was observed across the surface, with no visible cracking detected. At 300°C, specimens displayed early hairline cracking and slight reddish-grey discoloration, consistent with the onset of cement paste dehydration. At 400°C, micro-cracks became clearly visible and more widely distributed across the surface, while discoloration intensified to reddish-buff tones, attributable to the decomposition of calcium silicate hydrate and the oxidation of iron compounds within the aggregate [2,22]. At 500°C, specimens showed wide surface cracks, whitish-grey discoloration, and a friable texture, indicative of extensive microstructural disruption resulting from the decomposition of portlandite and significant reduction in paste integrity.

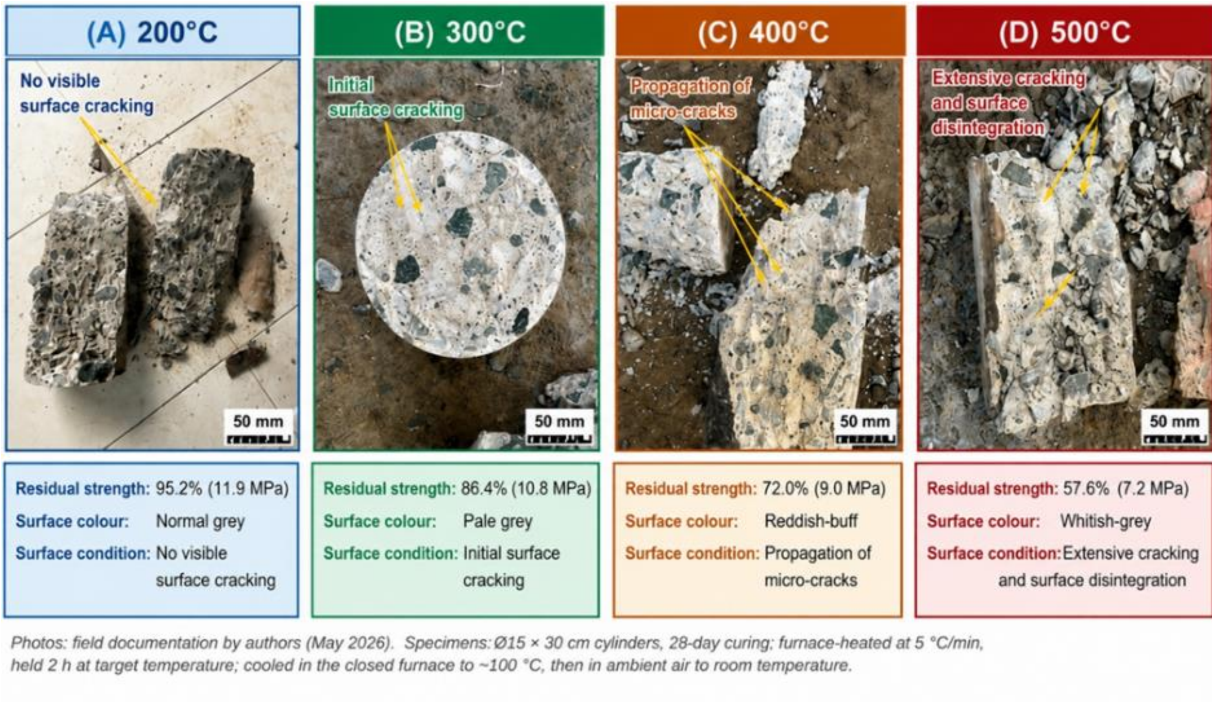

Fig. 4. Post-failure surface condition of low-strength concrete specimens (Ø15 × 30 cm cylinders) after exposure to elevated temperatures: (A) 200°C — normal grey, no visible cracks, 95.2% residual strength (11.9 MPa); (B) 300°C — pale grey, early hairline cracks, 86.4% residual strength (10.8 MPa); (C) 400°C — reddish-buff, visible micro-cracks, 72.0% residual strength (9.0 MPa); (D) 500°C — whitish-grey, wide cracks, friable texture, 57.6% residual strength (7.2 MPa). Photos: field documentation by authors (May 2026)

3.3 Non-Destructive Evaluation: Ultrasonic Pulse Velocity

Ultrasonic pulse velocity decreased progressively with increasing exposure temperature, mirroring the trend observed in residual compressive strength (Table 4). The unheated control recorded a pulse velocity of 3.27 km/s, graded as "medium" quality. Pulse velocity declined to 2.62 km/s at 200°C, 2.39 km/s at 300°C, and 2.22 km/s at 400°C — all falling within the "doubtful" quality band — before dropping further to 1.79 km/s at 500°C, graded as "poor" quality. This monotonic decline is consistent with the progressive microcracking and loss of matrix continuity discussed in Sections 4.1 and 4.2, since increased porosity and internal cracking reduce the stiffness-dependent propagation speed of ultrasonic waves through the concrete.

Table 4. Ultrasonic pulse velocity and quality grading of low-strength concrete after high-temperature exposure

Temperature	Mean Transit Time (µs)	Pulse Velocity (m/s)	Pulse Velocity (km/s)	Quality[1]
25°C (Control)	91.7	3272.7	3.27	Medium
200°C	114.7	2616.3	2.62	Doubtful
300°C	125.7	2387.3	2.39	Doubtful
400°C	135.3	2216.7	2.22	Doubtful
500°C	167.7	1789.3	1.79	Poor

[1] *Quality grading follows Whitehurst [41].*

The UPV trend corroborates the compressive strength results across the 200–500°C range tested, providing independent, non-destructive support for the strength degradation pattern reported in Section 3.1. Accordingly, the present findings support the integration of residual compressive strength testing with non-destructive evaluation, as previously recommended in the literature, to improve the reliability of post-fire structural assessment (Section 4.3). Nonetheless, because UPV quality grading was not independently calibrated against compressive strength for this specific mix, these results should be interpreted qualitatively, as a corroborating indicator of relative internal damage, rather than as a quantitative predictor of residual strength. The declining trend observed here is consistent with UPV–temperature relationships reported for other concrete grades: Kim et al. [42], testing normal- and lightweight-aggregate concretes (30–60 MPa) at 100–700°C, reported residual pulse velocities (relative to the unheated condition) of approximately 0.50–0.59 at 500°C, closely matching the residual pulse velocity of 0.547 (54.7%) obtained for the present low-strength concrete at the same temperature. Yang et al. [43] similarly demonstrated that UPV can track residual compressive strength degradation in heated concrete and proposed regression relationships between the two properties. This numerical agreement, obtained despite substantial differences in concrete grade and aggregate type, lends further support to the reliability of the UPV trend reported here, although mix-specific calibration would still be required for any quantitative strength prediction.

4. Discussions

4.1 Interpretation of Strength Degradation

The mechanistic interpretations offered in this section — including references to portlandite decomposition and calcium silicate hydrate (C–S–H) degradation — are inferential, drawn from thermochemical behavior established in the literature [2,3,20,22–24] and correlated with the residual strength loss and visual damage patterns observed here. No direct microstructural characterization (e.g., SEM, XRD, or TGA) was performed on the specimens in this study; these explanations should therefore be read as literature-informed hypotheses for the observed macroscopic behavior rather than as directly evidenced findings.

The experimental results clearly demonstrate a progressive reduction in residual compressive strength with increasing exposure temperature, confirming that elevated temperature significantly affects the physical and mechanical integrity of low-strength concrete, particularly beyond 300°C. Similar behavior has been widely reported in previous studies investigating fire-damaged concrete structures [2,3,22–25].

At 200°C, the 4.8% strength reduction indicates that the concrete matrix remained largely intact. The reduction is primarily associated with the evaporation of free and adsorbed water from capillary pores without significant decomposition of hydration products [2,3]. This finding is consistent with Khoury [22], who reported minimal strength loss below 250°C in ordinary Portland cement concrete. The absence of visible cracking supports this interpretation. Although Tukey's HSD post-hoc test indicated that this 4.8% reduction was statistically distinguishable from the control condition ($p < 0.001$, Section 3.1), owing to the very low within-group variability of the specimens, its practical engineering significance remains modest relative to the substantially larger losses recorded above 300°C.

More pronounced degradation at 300°C (13.6% reduction) reflects dehydration of calcium hydroxide and the initiation of microcracking within the interfacial transition zone [2,3]. At approximately 400–450°C, calcium hydroxide ($Ca(OH)_2$) decomposes into calcium oxide (CaO) and water vapor according to the reaction $Ca(OH)_2 \rightarrow CaO + H_2O$. This reaction increases internal porosity, weakens the cement paste, and promotes crack propagation. Differential thermal expansion between cement pastes and aggregates contributes to internal stress development, resulting in early crack propagation [20]. This threshold is broadly consistent with the findings of Phan and Carino [24] for normal-strength concrete, suggesting that the onset of chemically driven degradation occurs at similar temperatures across concrete grades. The present results also follow the probabilistic degradation trend reported by Shahraki et al. [2], who demonstrated that residual compressive strength decreases gradually below 300°C and accelerates significantly beyond approximately 400°C due to progressive decomposition of hydration products and thermal microcracking.

The most significant deterioration began at temperatures above 400°C, where residual compressive strength fell to 9.0 MPa (28.0% loss). This is likely attributable — based on thermochemical mechanisms established in the literature rather than direct microstructural evidence obtained in this study — to progressive decomposition of portlandite into calcium oxide and water vapor, which increases porosity and weakens paste cohesion [2,3]. Above approximately 500°C, calcium silicate hydrate (C–S–H), the principal binding phase responsible for concrete strength, progressively depolymerizes, resulting in severe loss of cohesion between aggregate particles. Similar reductions have been reported for CFRP-confined concrete systems [18] and concrete containing supplementary cementitious materials [19,33], confirming that $Ca(OH)_2$ decomposition is a dominant degradation driver across different concrete types. Wang et al. [11] also reported continuous strength degradation with increasing temperature in concrete with polypropylene fibres, although the fibres delayed crack propagation by improving pore pressure dissipation — consistent with Peng et al. [37], who showed that fibre toughening mitigates explosive spalling and helps preserve residual mechanical properties in high-performance concrete exposed to high temperatures. Similarly, the deterioration mechanisms observed herein are consistent with findings for concrete incorporating supplementary cementitious materials [19,33], indicating that temperature remains the dominant factor controlling residual strength regardless of binder modification. Although explosive spalling was not observed in the present low-strength concrete, the progressive crack development agrees with Hernandez-Figueirido et al. [10] and Mindeguia et al. [38], who demonstrated that thermal damage is governed by moisture migration and pore-pressure development. Abdulrazzaq et al. [32], publishing in Research on Engineering Structures and Materials, similarly reported compressive strength loss of 22.4% at 400°C and a more severe cumulative reduction of 79.3% at 800°C for normal-strength concrete (35 MPa), accompanied by visual observations of cracking and color change consistent with those documented in the present study. Kumar and Rajasekhar [34], also in Research on Engineering Structures and Materials, reported comparable residual strength trends for M20 grade concrete (approximately 20 MPa) exposed to 100–500°C, with no marked color change below 200°C but progressive discoloration and strength loss beyond 300°C, confirming that the degradation pattern observed in the present low-strength concrete ($f'c \approx 12.5$ MPa) is consistent with the behavior of similarly graded concrete in the international literature.

At 500°C, the 42.4% strength loss is associated with extensive decomposition of hydration products, intensified C–S–H depolymerization, and significant thermal incompatibility between concrete constituents [2,3,22]. The whitish-grey appearance and wide surface cracking observed at 500°C are consistent with severe dehydration, loss of cement-paste integrity, and extensive thermally induced cracking. The observed color transition from grey to reddish-grey and finally whitish-grey corresponds closely with the measured strength reduction. This suggests that visual inspection may provide a preliminary indication of residual structural condition before destructive testing is undertaken. These findings align with Kodur [23], Poon et al. [25], and Lau and Anson [29], who reported similar strength trajectories for heated concrete specimens.

Importantly, the rate of degradation observed in this study for low-strength concrete ($f'c \approx 12.5$ MPa) is broadly consistent with the general trends reported in the international literature for higher-grade concrete. This suggests that the fundamental physicochemical mechanisms governing thermal degradation are not strongly grade-dependent within the temperature range studied, although the absolute strength values and thus structural safety thresholds differ significantly between grades. Balaji et al. [33] confirmed a similar pattern for high-strength concrete (M50) with supplementary cementitious materials published in Research on Engineering Structures and Materials, reporting percentage reductions of 1.5% at 200°C, 4.8% at 400°C, and 20.8% at 600°C — indicating that while higher-grade concrete retains a greater margin of absolute strength, the relative degradation trajectory follows a comparable temperature-dependent pattern to that observed in the present low-strength concrete.

Table 5. Comparison of residual compressive strength at 500°C with selected international studies

Study	Concrete Grade	Temperature	Residual Strength
Khoury [22] (2000)	≈30 MPa	500°C	≈60%
Kodur [23] (2014)	35 MPa	500°C	≈58%
Shahraki et al. [2] (2023)	Review	500°C	55–65%
Present Study	12.5 MPa	500°C	57.6%

Similarly, visual changes to concrete color and cracking pattern systematically indicate the degree of thermal damage sustained. Table 6 summarizes the observed visual changes alongside residual strength values, providing a practical reference for field assessment.

Table 6. Visual observations and residual strength at each temperature level

Temperature	Color	Cracking	Condition	Residual Strength
25°C (Control)	Grey	None	Intact	100% (12.5 MPa)
200°C	Light grey	None	Intact	95.2% (11.9 MPa)
300°C	Reddish-grey	Hairline	Minor damage	86.4% (10.8 MPa)
400°C	Reddish-buff	Micro-crack	Moderate damage	72.0% (9.0 MPa)
500°C	Whitish-grey	Wide crack	Severe / friable	57.6% (7.2 MPa)

4.2 Literature-Based Interpretation of Residual Strength Reduction and Mineralogical Changes

Although X-ray diffraction (XRD) analysis was not performed in the present investigation, the experimentally observed deterioration trend is consistent with mineralogical transformations widely reported in previous studies. XRD has been extensively employed to characterize phase changes occurring in cementitious materials subjected to elevated temperatures, providing valuable insight into the mechanisms responsible for the degradation of concrete mechanical properties [2,3,20,22,23,35,36]. At ambient temperature, hydrated cement paste is primarily composed of calcium silicate hydrate (C–S–H), portlandite ($Ca(OH)_2$), ettringite, and minor quantities of calcite and quartz originating from the aggregates [20,22]. Among these phases, C–S–H is the principal contributor to concrete strength, whereas portlandite contributes to the alkalinity and stability of the cement matrix.

Exposure to temperatures below approximately 200°C generally produces only minor changes in XRD diffraction patterns. Previous studies have shown that the principal crystalline phases remain largely unchanged, while moisture evaporation and dehydration of physically bound water constitute the dominant deterioration mechanisms [3,20,36]. Consistent with this, the present study observed only a modest compressive strength reduction of approximately 4.8% at 200°C, indicating that the cementitious matrix remained relatively intact.

As the exposure temperature increased to 300–400°C, progressive dehydration of C–S–H gel and decomposition of portlandite became increasingly significant. XRD analyses reported by previous researchers consistently demonstrate a gradual reduction in the intensity of portlandite diffraction peaks within this temperature range, indicating decomposition of calcium hydroxide into calcium oxide and water vapor [2,3,22,23,36]. Simultaneously, partial degradation of the C–S–H structure reduces cohesion within the cement paste and weakens the interfacial transition zone (ITZ) between the aggregate and the surrounding matrix [2,20]. These mineralogical transformations correspond well with the approximately 28.0% reduction in residual compressive strength observed at 400°C in the present experimental program.

At 500°C, the deterioration process becomes substantially more severe. Numerous XRD investigations have reported that portlandite peaks almost disappear, reflecting extensive decomposition of calcium hydroxide [22,23,30,35]. Furthermore, dehydration of C–S–H becomes more pronounced, resulting in increased porosity, loss of matrix continuity, and progressive formation of interconnected microcracks [2,3]. These physicochemical changes are broadly consistent with the severe surface cracking and approximately 42.4% reduction in residual compressive strength measured in this study.

Table 7 summarizes the typical mineralogical evolution of concrete subjected to elevated temperatures, synthesized from previously published XRD studies, to support interpretation of the experimental compressive strength results obtained in the present investigation.

Table 7. Typical mineralogical evolution of concrete subjected to elevated temperatures based on previous XRD studies

Temperature	Typical XRD Observations	Mechanical Implication
Ambient	Strong peaks of portlandite, C–S–H, quartz	Normal mechanical properties
100–200°C	No significant phase transformation; evaporation of free water	Slight strength reduction
300–400°C	Progressive decrease of portlandite peaks; partial dehydration of C–S–H	Moderate strength loss and initiation of microcracking
500°C	Extensive decomposition of portlandite; severe C–S–H degradation	Significant strength reduction, extensive cracking and spalling
>600°C	Formation of high-temperature reaction products; substantial matrix deterioration	Severe structural degradation

Note: The mineralogical changes summarized in this table are synthesized from previously published XRD studies [2,3,20,22,23,30,35,36] and are presented to support interpretation of the experimental compressive strength results obtained in the present investigation; no XRD measurements were performed in this study.

Although the present investigation did not directly verify these mineralogical transformations through XRD measurements, the close agreement between the experimentally observed mechanical deterioration and the mineralogical evolution reported in previous studies suggests that similar degradation mechanisms plausibly governed the behavior of the tested low-strength concrete. This interpretation remains a literature-informed hypothesis rather than a directly evidenced finding; direct microstructural verification (XRD, SEM, mercury intrusion porosimeter) is identified as a priority for future work in Section 4.5.

4.3 Structural Implications and Post-Fire Assessment

From a structural engineering perspective, the 28% strength loss recorded at 400°C exceeds the indicative 20–25% serviceability threshold adopted in this study [2,4,15,26], indicating that concrete exposed to this temperature cannot be considered fully serviceable without detailed evaluation and possible strengthening measures. Studies on fire-damaged reinforced concrete columns have similarly suggested that structural repair and strengthening become necessary once significant thermal degradation has occurred [17]; fundamental principles governing the interaction between reinforcement and heat-damaged concrete, including the reduction of bond and confinement effectiveness at elevated temperature, are described in detail by Guo [39].

It should be emphasized that these observations concern material-level degradation of plain, unreinforced concrete cylinders (150 × 300 mm) tested under controlled laboratory conditions. Actual post-fire structural capacity also depends on reinforcement condition, member scale, restraint, and connectivity, none of which were evaluated in this study. Accordingly, the strength-loss thresholds discussed here should inform, rather than substitute for, member-level structural assessment; they do not, by themselves, justify a demolition decision for any specific structure.

The degradation mechanisms identified also have important implications for structural behavior during actual fire scenarios. Previous investigations on localized fire exposure in reinforced concrete buildings reported that thermal expansion may induce substantial slab displacement and redistribution of internal forces [16]. Such thermally induced deformation may further increase the vulnerability of fire-damaged structures, especially in older buildings constructed using low-strength concrete.

The findings are particularly relevant for post-fire assessment of school buildings and public facilities in Indonesia, where low-strength concrete is commonly encountered. Structures exposed to temperatures approaching 500°C may experience severe reductions in load-bearing capacity even when external damage appears visually moderate. Therefore, residual compressive strength testing should be combined with visual inspection and non-destructive evaluation methods — such as ultrasonic pulse velocity and rebound hammer testing — to improve reliability of post-fire safety assessment [5,6]. The UPV results obtained in the present study (Section 3.3) illustrate this complementary role directly: pulse velocity declined progressively from 3.27 km/s (control, "medium" quality) to 1.79 km/s at 500°C ("poor" quality), corroborating the compressive strength trend using an independent, non-destructive method.

4.4 Relation to the SDN 022 Penajam Fire Incident

The laboratory findings provide an empirically grounded interpretation of the fire damage observed at SD Negeri 022 Penajam. The severe structural deterioration documented — including extensive surface cracking, spalling, and visible discoloration of structural elements — plausibly corresponds to in-situ temperature exposure exceeding 400°C, at which the present experimental program recorded substantial compressive strength degradation of 28.0% or greater. At 500°C, specimens exhibited a cumulative strength loss of 42.4%, accompanied by wide surface cracking and whitish-grey discoloration characteristic of advanced microstructural breakdown. These observations are broadly consistent with the physical condition of the fire-affected structural members reported at the site.

Although the laboratory simulation cannot fully replicate the complex thermal conditions of a real building fire — which may involve non-uniform heat distribution, variable fire duration, localized hot spots, differential cooling rates, and the influence of applied loading — the experimental results remain contextually relevant. Consequently, the temperature exposures applied should be understood as representative thermal benchmarks rather than precise replications of the fire event.

The laboratory results are qualitatively consistent with the severity of damage observed at SDN 022 Penajam. However, they should not be interpreted as direct verification of the in-situ temperature exposure, residual structural capacity, or demolition decision. A definitive post-fire assessment would require member-level capacity analysis, core extraction and testing, and a comprehensive evaluation of reinforcement condition.

4.5 Limitations and Future Research

Several limitations should be acknowledged. First, newly cast laboratory specimens were used instead of concrete cores extracted from the fire-damaged building, introducing uncertainty regarding exact correspondence with in-situ properties. Second, the sample size of three specimens per temperature group restricts statistical robustness; future studies should use $n \geq 5$ per group to achieve adequate statistical power. Third, the study focused on residual compressive strength and visual observations without conducting detailed microstructural analyses such as scanning electron microscopy (SEM), X-ray diffraction (XRD), or mercury intrusion porosimeter (MIP). Fourth, the furnace-based heating protocol does not fully replicate the heating and cooling dynamics of a real compartment fire.

Future studies should therefore investigate broader concrete strength ranges (f'c 15–25 MPa) as a transition class, incorporate supplementary cementitious materials commonly used in Indonesia (fly ash, rice husk ash), and perform advanced microstructural characterization to better explain thermal degradation mechanisms. The present study incorporated ultrasonic pulse velocity (UPV) as a first non-destructive corroboration (Section 3.3); however, UPV alone could not be independently calibrated against compressive strength for this specific mix. Future work should therefore pair UPV with rebound hammer (Schmidt hammer) testing in a combined SonReb approach, and expand UPV measurement to a larger specimen set, to develop a mix-specific, calibrated non-destructive prediction model for low-strength concrete post-fire assessment.

5. Conclusion

- Residual compressive strength declined monotonically with increasing temperature, from a control mean of 12.5 MPa at 25°C to 7.2 MPa at 500°C, representing a cumulative loss of 42.4%. Intermediate reductions of 4.8%, 13.6%, and 28.0% were recorded at 200°C, 300°C, and 400°C, respectively. One-way ANOVA confirmed a statistically significant overall temperature effect ($F(4,10) = 1015.07$, $p < 0.001$), and Tukey's HSD post-hoc tests showed that every pairwise comparison, including control versus 200°C, was statistically significant, reflecting the very low within-group variability of the tested specimens. Given the small sample size ($n = 3$ per group), these findings should be regarded as indicative and confirmed through larger experimental program.
- The rate of strength decline accelerated markedly above 300°C, consistent with the progressive onset of thermally induced physicochemical deterioration: $Ca(OH)_2$ decomposition at approximately 300–400°C, C–S–H breakdown, and intensified microcracking from thermal-expansion mismatch between cement paste and aggregates.
- Visual observations confirmed a systematic progression in surface damage: no cracking at 200°C, early hairline cracks and slight discoloration at 300°C, visible micro-cracks and reddish-buff discoloration at 400°C, and wide cracks with whitish-grey friable surface at 500°C.
- At the material level, low-strength concrete exposed to temperatures of ≥ 400°C exhibited substantial residual strength loss (≥ 28%) that exceeds commonly adopted serviceability thresholds. Because the specimens tested were plain, unreinforced cylinders, these findings characterize material-level degradation rather than in-situ structural capacity; reinforcement condition, member scale, restraint, and connectivity also govern actual structural safety and were outside the scope of this study. Post-fire assessment of concrete elements exposed to such temperatures should therefore encompass residual compressive strength testing of extracted cores, visual and non-destructive inspection, and member-level structural capacity analysis performed by a qualified structural engineer before any decision on repair, strengthening, or demolition is made.
- The laboratory findings provide contextual, material-level evidence consistent with the severity of damage observed at SDN 022 Penajam. However, this study does not constitute a formal structural safety assessment of the building and cannot independently validate the demolition decision.
- Ultrasonic pulse velocity (UPV), used as an independent non-destructive check, declined progressively from 3.27 km/s (control, "medium" quality) to 1.79 km/s at 500°C ("poor" quality), corroborating the compressive strength degradation trend and aligning closely with UPV–temperature relationships reported for other concrete grades in the literature. This agreement supports the combined use of destructive and non-destructive methods for post-fire assessment of low-strength concrete.
- These findings provide a locally grounded empirical reference for post-fire structural assessment of low-grade concrete in the Indonesian context, where such data remain scarce. The findings should be treated as indicative pending confirmation through larger-scale experimental program.

Acknowledgement

The authors express sincere gratitude to the Department of Education of Penajam Paser Utara Regency for their collaboration and support in allowing this study to be conducted prior to the demolition of the fire-damaged elementary school building.

References

[1] Badan Pusat Statistik (BPS). Konstruksi dalam Angka 2023. Jakarta: BPS; 2023.

[2] Shahraki M, Hua N, Elhami-Khorasani N, Tessari A, Garlock M. Residual compressive strength of concrete after exposure to high temperatures: A review and probabilistic models. Fire Saf J. 2023;135:103698. https://doi.org/10.1016/j.firesaf.2022.103698

[3] Kakae N, Miyamoto K, Momma T, Sawada S, Kumagai H, Ohga Y, et al. Physical and thermal properties of concrete subjected to high temperature. J Adv Concr Technol. 2017;15(6):190-212. https://doi.org/10.3151/jact.15.190
[4] Kodur VKR, Agrawal A. An approach for evaluating residual capacity of reinforced concrete beams exposed to fire. Eng Struct. 2016;110:293-306. https://doi.org/10.1016/j.engstruct.2015.11.047
[5] Alcaino P, Santa-Maria H, Magna-Verdugo C, Lopez L. Experimental fast-assessment of post-fire residual strength of reinforced concrete frame buildings based on non-destructive tests. Constr Build Mater. 2020;234:117371. https://doi.org/10.1016/j.conbuildmat.2019.117371
[6] Park GK, Yim HJ. Evaluation of fire-damaged concrete: An experimental analysis based on destructive and nondestructive methods. Int J Concrete Struct Mater. 2017;11(3):447-457. https://doi.org/10.1007/s40069-017-0205-2
[7] Kerr T, Vetter M, Gonzalez-Rodriguez J. Evaluating residual compressive strength of post-fire concrete using Raman spectroscopy. Forensic Sci Int. 2021;325:110874. https://doi.org/10.1016/j.forsciint.2021.110874
[8] Timilsina S, Yazdani N, Beneberu E. Post-fire analysis and numerical modeling of a fire-damaged concrete bridge. Eng Struct. 2021;244:112764. https://doi.org/10.1016/j.engstruct.2021.112764
[9] Hager I, Mroz K. Role of polypropylene fibres in concrete spalling risk mitigation in fire and test methods of fibres effectiveness evaluation. Materials. 2019;12(23):3869. https://doi.org/10.3390/ma12233869
[10] Hernandez-Figueirido D, Paya-Zaforteza I, Hospitaler A, Teran-Aguilar D. Spalling phenomenon and fire resistance of ultrahigh-performance concrete. Constr Build Mater. 2024;443:137695. https://doi.org/10.1016/j.conbuildmat.2024.137695
[11] Wang Y, Nejati F, Edalatpanah SA, Karim RG. Experimental study to compare the strength of concrete with different amounts of polypropylene fibers at high temperatures. Sci Rep. 2024;14(1):8566. https://doi.org/10.1038/s41598-024-59008-0
[12] Al-Ameri RA, Abid SR, Ozakca M. Mechanical and impact properties of engineered cementitious composites reinforced with PP fibers at elevated temperatures. Fire. 2022;5(1):3. https://doi.org/10.3390/fire5010003
[13] Al-Ameri RA, Abid SR, Murali G, Ali SH, Ozakca M. Residual repeated impact strength of concrete exposed to elevated temperatures. Crystals. 2021;11(8):941. https://doi.org/10.3390/cryst11080941
[14] Badan Standardisasi Nasional (BSN). SNI 1974:2011: Cara Uji Kuat Tekan Beton dengan Benda Uji Silinder. Jakarta: BSN; 2011.
[15] British Standards Institution (BSI). Eurocode 2: Design of Concrete Structures - Part 1-2: General Rules - Structural Fire Design (BS EN 1992-1-2:2004+A1:2019). London: BSI; 2019.
[16] Murtiadi S, Akmaluddin A. Performance of concrete building structure exposed to localized fire. Civ Eng Archit. 2023;11(1):114-122. https://doi.org/10.13189/cea.2023.110110
[17] Kareem MM, Mohammed HA, Abdulhameed AA. Repair of fire damaged axially loaded short RC columns using CFRP sheets. Civ Eng Archit. 2021;9(6):1936-1945. https://doi.org/10.13189/cea.2021.090624
[18] Mohammed AA, Kareem MM. Compressive strength of CFRP confined concrete under exposure to high temperature. Civ Eng Archit. 2021;9(5A):68-75. https://doi.org/10.13189/cea.2021.091308
[19] Al-Jabri AS, Al-Salloum YA, Almusallam TH, Al-Haddad MS. Effect of high elevated temperature on the behavior of concrete containing slag and nano clay. Civ Eng Archit. 2025;13(3). https://doi.org/10.13189/cea.2025.130301
[20] Ulm FJ, Coussy O, Bazant ZP, Wittmann FH. Thermo-hygro-mechanical behavior of concrete at high temperatures. Cem Concr Res. 1999;29(4):537-544. https://doi.org/10.1016/S0008-8846(99)00008-2
[21] Kalifa P, Chene G, Galle C. High-temperature behaviour of HPC with polypropylene fibres: From spalling to microstructure. Cem Concr Res. 2001;31(10):1487-1499. https://doi.org/10.1016/S0008-8846(01)00596-8
[22] Khoury GA. Effect of fire on concrete and concrete structures. Prog Struct Eng Mater. 2000;2(4):429-447. https://doi.org/10.1002/pse.51
[23] Kodur VKR. Properties of concrete at elevated temperatures. ISRN Civ Eng. 2014;2014:468510. https://doi.org/10.1155/2014/468510
[24] Phan LT, Carino NJ. Review of mechanical properties of HSC at elevated temperature. J Mater Civ Eng. 1998;10(1):58-65. https://doi.org/10.1061/(ASCE)0899-1561(1998)10:1(58
[25] Poon CS, Azhar S, Anson M, Wong YL. Strength and durability recovery of fire-damaged concrete after post-fire-curing. Cem Concr Res. 2001;31(9):1307-1318. https://doi.org/10.1016/S0008-8846(01)00582-8
[26] Buchanan AH, Abu AK. Structural Design for Fire Safety. 2nd ed. Chichester: Wiley; 2017. https://doi.org/10.1002/9781118700402
[27] Ali F, Nadjai A, Silcock G, Abu-Tair A. Outcomes of a major research on fire resistance of concrete columns. Fire Saf J. 2004;39(6):433-445. https://doi.org/10.1016/j.firesaf.2004.02.004

[28] Hertz KD. Concrete strength for fire design. Mag Concr Res. 2005;57(8):445-453. https://doi.org/10.1680/macr.2005.57.8.445
[29] Lau A, Anson M. Effect of high temperatures on high performance steel fibre reinforced concrete. Cem Concr Res. 2006;36(9):1698-1707. https://doi.org/10.1016/j.cemconres.2006.03.024
[30] Bazant ZP, Kaplan MF. Concrete at High Temperatures: Material Properties and Mathematical Models. London: Longman; 1996.
[31] Tamrin, Nurdiana J. The effect of recycled HDPE plastic additions on concrete performance. Recycling. 2021;6(1):18. https://doi.org/10.3390/recycling6010018
[32] Abdulrazzaq AM, Abdulhameed HA, Hassan MS. Effects of elevated temperatures on the stress-strain behavior and microstructure of normal and high-strength concrete. Res Eng Struct Mater. 2025. https://doi.org/10.17515/resm2025-1260ic1013rs
[33] Balaji T, Jeyashree TM, Kannan Rajkumar PR, Baskara Sundararaj J, Jegan M. Effect of elevated temperature on concrete incorporating zeolite, silica fume and fly ash as replacement for cement. Res Eng Struct Mater. 2025;11(3):1245-1258. https://doi.org/10.17515/resm2024.267ma0506rs
[34] Kumar GP, Rajasekhar K. Influence of elevated temperatures on M20 grade concrete with colloidal silica. Res Eng Struct Mater. 2025. https://doi.org/10.17515/resm2025-965ma0614rs
[35] Phan LT. Fire Performance of High-Strength Concrete: A Report of the State-of-the-Art. NISTIR 5934. Gaithersburg: National Institute of Standards and Technology; 1996. https://doi.org/10.6028/NIST.IR.5934
[36] Hager I. Behaviour of cement concrete at high temperature. Bull Polish Acad Sci Tech Sci. 2013;61(1):145-154. https://doi.org/10.2478/bpasts-2013-0013
[37] Peng GF, Yang WW, Zhao J, Liu YF, Bian SH, Zhao LH. Explosive spalling and residual mechanical properties of fiber-toughened high-performance concrete subjected to high temperatures. Cem Concr Res. 2006;36(4):723-727. https://doi.org/10.1016/j.cemconres.2005.12.014
[38] Mindeguia JC, Pimienta P, Noumowe A, Kanema M. Temperature, pore pressure and mass variation of concrete subjected to high temperature — experimental and numerical discussion on spalling risk. Cem Concr Res. 2010;40(3):477-487. https://doi.org/10.1016/j.cemconres.2009.10.011
[39] Guo Z. Principles of Reinforced Concrete. Oxford: Elsevier/Tsinghua University Press; 2014. https://doi.org/10.1016/B978-0-12-800054-0.00001-X
[40] ASTM International. ASTM C597-16: Standard Test Method for Pulse Velocity Through Concrete. West Conshohocken: ASTM International; 2016. https://doi.org/10.1520/C0597-16
[41] Whitehurst EA. Soniscope tests concrete structures. J Am Concr Inst. 1951;47:433-444. https://doi.org/10.14359/12002
[42] Kim W, Choi H, Lee T. Residual compressive strength prediction model for concrete subject to high temperatures using ultrasonic pulse velocity. Materials. 2023;16(2):515. https://doi.org/10.3390/ma16020515
[43] Yang H, Lin Y, Hsiao C, Liu JY. Evaluating residual compressive strength of concrete at elevated temperatures using ultrasonic pulse velocity. Fire Saf J. 2009;44(1):121-130. https://doi.org/10.1016/j.firesaf.2008.05.003